

# Bioinformatics and Molecular Docking Study of $\beta$ -Glucosidase J384W Locus Mutation

Hong Pan\*, Xiangyu Yao, Yinan Hong, Xiaojun Wang, Yurou Fan

School of Environmental and Chemical Engineering, Xi'an Polytechnic University, Xi'an 710048, China

\*Corresponding author: Hong Pan, 441595837@qq.com

**Copyright:** © 2023 Author(s). This is an open-access article distributed under the terms of the Creative Commons Attribution License (CC BY 4.0), permitting distribution and reproduction in any medium, provided the original work is cited.

## Abstract:

To improve the conversion efficiency of ginsenoside Rb1 by  $\beta$ -glucosidase, the key regions and sites involved in substrate recognition and binding were obtained through molecular docking during the conversion of ginsenoside Rb1 by  $\beta$ -glucosidase. The J384 site was subject to site-directed mutation to W384, and the physicochemical properties, hydrophilicity/hydrophobicity, transmembrane regions, and secondary/tertiary structures of the wild-type and mutant enzymes were compared using bioinformatics. The results showed that modifying the internal structure of the enzyme increased the number of binding sites and enhanced overall stability. The mutant enzyme was more likely to spontaneously bind to ginsenoside Rb1 than the wild-type enzyme, with a minimum binding energy of -9.02 kJ/mol.

## Keywords:

$\beta$ -glucosidase  
Site-directed mutation  
Bioinformatics  
Molecular docking

**Online publication:** December 22, 2023

## 1. Introduction

$\beta$ -glucosidase is a crucial component of cellulase<sup>[1]</sup>, primarily involved in cellulose metabolism and various biochemical pathways. The low catalytic efficiency of the enzyme and the slow enzymatic conversion rate of glucose are attributed to the feedback inhibition of glucose. Therefore, engineering  $\beta$ -glucosidase is essential for producing enzymes with high catalytic efficiency<sup>[2]</sup>. In the production of second-generation biofuels,  $\beta$ -glucosidase plays a role in the final step of saccharification, cleaving the  $\beta$ -1,4 glycosidic bond of cellobiose to produce glucose molecules<sup>[3]</sup>.

However,  $\beta$ -glucosidase is strongly inhibited by glucose, leading to increased concentrations of glucanase and endoglucanase<sup>[4]</sup>. The characterization and improvement of  $\beta$ -glucosidase have been research goals in recent years, aiming to enhance sugar tolerance and thermal stability. By reviewing relevant literature on  $\beta$ -glucosidase<sup>[5,6]</sup>, it has been found that changes at the J384 site have an impact on  $\beta$ -glucosidase. In this study, important sites within the active pocket were selected for site-directed mutagenesis. Through bioinformatics and molecular docking techniques, the structure and properties of wild-type  $\beta$ -glucosidase were compared with those of the

mutant protein to analyze the molecular mechanism of  $\beta$ -glucosidase involved in the transformation of ginsenoside Rb1.

## 2. Materials and methods

### 2.1. Bioinformatics comparison

The gene and amino acid sequences of the hydrolase  $\beta$ -glucosidase (ID: 3WH7) were downloaded from the RCSB database website (<https://www.rcsb.org/>)<sup>[7,8]</sup>. The physicochemical properties and stability of  $\beta$ -glucosidase were analyzed using ProtParam software. ProtScale and Tmhmm were used to predict the hydrophilicity/hydrophobicity and transmembrane regions of the protein, respectively. PredictProtein and Swiss-Model online software were used to predict and analyze the secondary and tertiary structures of the protein.

### 2.2. Molecular docking

Autodock 4.2.6 and Autodock Tools 1.5.7 software were downloaded from the Autodock software official website (<http://autodock.scripps.edu/>)<sup>[9]</sup>. The 3D structure program database file of hydrolase  $\beta$ -glucosidase was downloaded from the PDB database, consistent with the enzyme used in bioinformatics. The small molecule structure SDF file of ginsenoside Rb1 was downloaded from the Pubmed database and converted to PDB format using Openbabel software. The downloaded  $\beta$ -glucosidase file was imported into Autodock, and the protein receptor was dehydrated and hydrogenated. Due to the high uncertainty of flexible groups, semi-flexible docking was chosen. The ligand was read in Autodock, and non-polar hydrogen atoms were merged and added with Gasteiger charges to maintain a minimum energy state<sup>[10]</sup>. The position and number of small molecule centers and rotatable bonds were viewed through the Ligand subroutine package. The file was saved as Rb1.pdbqt. Molecular docking was performed using AntodockVina software to obtain the initial coordinates of the ligand-receptor complex (40.518, 29.090, 8.272)<sup>[11,12]</sup>. The docking box size was set within a reasonable range to completely enclose the volume of the entire substrate catalytic site, with a grid spacing of 0.2983 Å. A semi-empirical scoring function, Lamarckian genetic algorithm<sup>[13]</sup>, and semi-flexible docking algorithm were used during

the ligand conformation search process. The number of rounds for molecular docking was set to 50, and all other parameters were set to default values.

## 3. Results and analysis

### 3.1. Physicochemical properties of wild-type and mutant enzymes

The physicochemical properties of two  $\beta$ -glucosidases were predicted using ProtParam software, and the wild-type  $\beta$ -glucosidase was compared with the mutant  $\beta$ -glucosidase<sup>[14]</sup>. The wild-type enzyme consists of 451 amino acids with a relative molecular weight of approximately 49.13 kD. The isoelectric point of the protein is 4.88, and the instability coefficient of the wild-type enzyme is 32.58, which is less than 40. According to the criterion for judging the instability index, the wild-type enzyme is a stable protein. Additionally, the average hydrophobicity index of the wild-type  $\beta$ -glucosidase is -0.220, indicating that it is a hydrophilic protein.

Prediction of the mutant  $\beta$ -glucosidase showed that it consists of 450 amino acids. Its relative molecular weight is approximately the same as that of the wild-type enzyme, around 49.18 kD. The isoelectric point of the protein is 3.57. The average hydrophobicity index of the mutant enzyme is -0.214, and the instability coefficient is 32.37, which is less than 40. Compared with the wild-type enzyme, the mutant enzyme has a lower instability coefficient, indicating that the site mutation did not change the protein's hydrophilicity/hydrophobicity. However, the mutant enzyme has a lower average hydrophobicity index and a smaller stability index compared to the wild-type enzyme, suggesting stronger protein stability.

The comparison results between the wild-type and mutant enzymes were visualized using software, and the amino acid statistics of the wild-type and mutant enzymes are shown in **Table 1**.

It can be observed that compared to the wild enzyme, the mutant enzyme has an increase of 2 amino acids in both the aliphatic and aromatic categories. The number of amino acids with alcoholic hydroxyl groups has also risen, while the counts of sulfur-containing, basic, and acidic amino acids have decreased. Changes in the number of amino acid types have led to variations

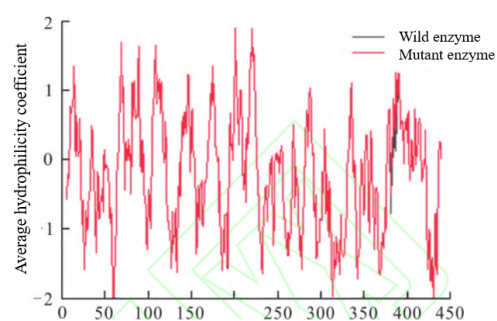
**Table 1.** Amino acid statistics of wild-type and mutant enzymes

Types of amino acids	Wild enzyme (piece)	Mutant enzyme (piece)	Wild enzyme (%)	Mutant enzyme (%)
Aliphatic	186	188	41.24	41.78
Aromatic	51	52	11.31	11.56
Sulfur-containing	14	13	3.1	2.89
Basic	49	48	10.86	10.67
Acidic	89	87	19.73	19.33
Alcoholic hydroxyl group	32	33	7.1	7.33

in the total amino acid count of the protein, resulting in a lower total amino acid count for the mutant enzyme compared to the wild enzyme. Additionally, both aliphatic and aromatic amino acids belong to the group of amino acids with non-polar and hydrophobic R-groups. The increase in these two types of amino acids in the mutant enzyme suggests an enhanced hydrophobicity compared to the wild enzyme.

### 3.2. Hydrophilicity/Hydrophobicity comparison

The hydrophilicity/hydrophobicity analysis of the two  $\beta$ -glucosidase enzymes was conducted using the online prediction platform ProtScale (<https://web.expasy.org/protscale>)<sup>[15,16]</sup>. The results indicated that the most hydrophilic site of both  $\beta$ -glucosidase proteins is the arginine at position 60, with a score of -2.444. The most hydrophobic sites are histidine at position 201 and isoleucine at position 220, with a score of 1.911. The distribution of hydrophilic/hydrophobic peptide chains in the enzyme protein sequence suggests that it is a hydrophilic protein. The most hydrophilic/hydrophobic sites of the mutant enzyme remain unchanged, and a comparison of hydrophilicity/hydrophobicity is shown in

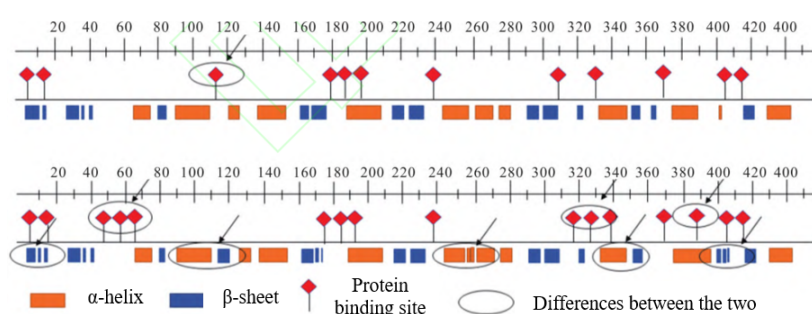
**Figure 1.** Affinity/hydrophobicity comparison.

**Figure 1.** It can be seen that after site mutation, there is no significant change in the hydrophilicity/hydrophobicity of  $\beta$ -glucosidase. However, the scores of the mutant enzyme at positions 381–387 are higher than those of the wild enzyme, indicating a slight increase in hydrophilicity in this region.

### 3.3. Secondary structure prediction

The secondary structure prediction of the wild enzyme was performed using the online prediction platform SOPMA (<http://npsa-pbil.ibcp.fr/>)<sup>[17]</sup>. The comparative analysis of the secondary structure prediction results is shown in **Figure 2**.

It can be seen that the protein contains 12  $\alpha$ -helices and 16  $\beta$ -sheets, with amino acid ratios of 38.15% and 15.35% for  $\alpha$ -helices and  $\beta$ -sheets, respectively. The mutant enzyme has 21  $\alpha$ -helices and 12  $\beta$ -sheets. In the 3–45 site region, the wild enzyme forms 5 helical regions (3–11, 13–14, 27–32, 35–36, 39–41), while the mutant enzyme forms 6 helical regions (3–6, 8–9, 10–11, 23–26, 37–38, 39–40). At the 80–83 site, both the wild and mutant enzymes generate one helical region each; at the 118–122 site, the mutant enzyme generates one

**Figure 2.** Comparison of secondary structure analysis.

helical region. Additionally, there are changes in binding sites. The wild enzyme has 12 binding sites, while the mutant enzyme has 16 binding sites, an increase of 4 sites compared to the wild enzyme.

### 3.4. Tertiary structure prediction

Homology modeling of wild-type  $\beta$ -glucosidase and mutant  $\beta$ -glucosidase was performed using the online prediction platform SwissModel (<https://swissmodel.expasy.org/>)<sup>[18]</sup>. The amino acid sequences of the two  $\beta$ -glucosidase proteins show similar wave patterns to their respective model proteins. The wave patterns of the protein structures are relatively stable, and most of the amino acid residue scores are higher than 0.6, indicating that the predicted models are close to the real situation.

Changes in the tertiary structure steric hindrance of the mutant  $\beta$ -glucosidase were analyzed and predicted using Swiss-PdbViewer 4.1.0 software<sup>[19]</sup>. The tertiary structure space is shown in **Figure 3**.

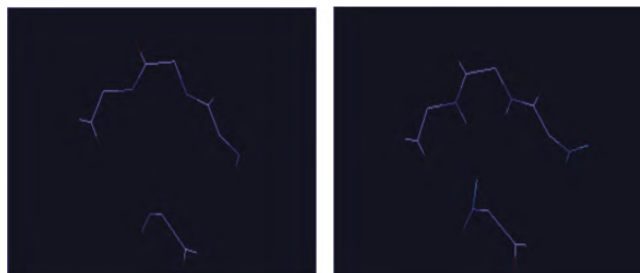


**Figure 3.** Three-level structural space diagram.

It can be observed that after the mutation of  $\beta$ -glucosidase, there is an increase in hydrogen bonds formed by side chain groups. The spatial position occupied by the atomic side chains near the reaction center becomes larger, increasing the steric hindrance. Overall, the structure tends to be more stable and intact. Following the mutation of  $\beta$ -glucosidase, there are also changes in the internal spatial structure. The statistics of the dihedral angles of the four amino acids are shown in **Table 2**.

It can be seen that the  $\phi$ <sup>[20]</sup> value decreases slightly, while the  $\psi$ <sup>[21]</sup> value remains unchanged. This suggests that there are changes in internal spatial structure after mutation, but the magnitude of these changes is relatively small. The  $\phi$  of an amino acid refers to the dihedral angle between the four atoms: the C atom of the

adjacent amino acid, and the N, CA, and C atoms of the amino acid itself. The  $\psi$  of an amino acid refers to the dihedral angle between the four atoms: the N, CA, and C atoms of the amino acid, and the N atom of the adjacent amino acid<sup>[22]</sup>.

**Table 2.** Statistics of dihedral angles of four amino acids

Site	Wave function			
	$\phi$		$\psi$	
	Wild type	Mutant type	Wild type	Mutant type
GLY3	47.406	47.392	36.011	36.000
	41.294	41.286	11.640	11.640
GLU4	49.611	49.625	33.693	33.631
	42.838	42.860	13.020	13.020
ARG5	51.066	50.974	31.269	31.261
	40.634	40.605	10.930	10.930
GLN384	43.671	43.673	30.899	30.982
	37.476	37.455	6.070	6.070

### 3.5. Docking results of $\beta$ -glucosidase with ginsenoside Rb1

Two sets of docking experiments each output 50 docking result conformations. All conformations are arranged in order of increasing energy, and binding constants are calculated based on the top 10 lowest-energy docking models and their scoring. The slight decrease in  $\phi$ <sup>[20]</sup> value and no change in  $\psi$ <sup>[21]</sup> value indicate that there are changes in the internal spatial structure after mutation, but the magnitude of these changes is small. A comparison of the docking models is shown in **Table 3**.

It can be observed that the Gibbs free energy of all docking models is less than 0, indicating that both wild-type and mutant  $\beta$ -glucosidase can spontaneously interact with ginsenoside Rb1. The lowest binding energy value between wild-type  $\beta$ -glucosidase and ginsenoside Rb1 is -5.93 kJ/mol, while the lowest binding energy value between mutant  $\beta$ -glucosidase and ginsenoside Rb1 is -9.02 kJ/mol. The binding constant value of the mutant enzyme with ginsenoside Rb1 is higher than that of the wild-type enzyme, indicating a stronger interaction between the mutant  $\beta$ -glucosidase and ginsenoside Rb1.

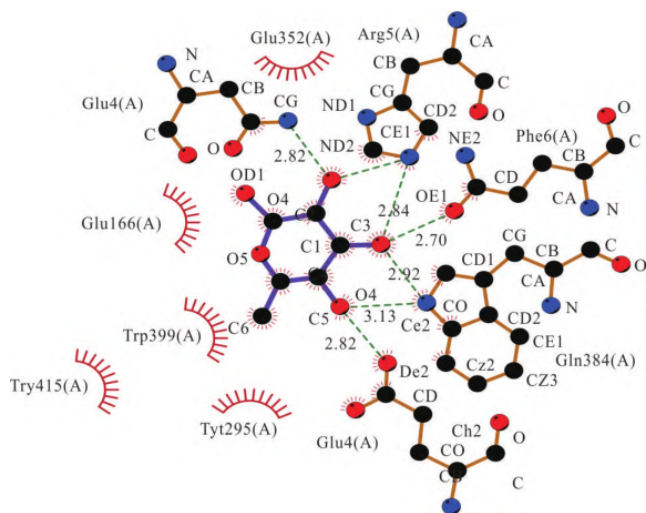


**Table 3.** Comparison of wild-type and mutant-type docking models

Gibbs free energy (kJmol)		Wild type mutant type binding constant (10,000 Kamol <sup>-1</sup> L <sup>-1</sup> )	
Wild type	Mutant type	Wild type	Mutant type
-5.39	-9.02	35.98	36.36
-5.37	-8.88	35.06	35.35
-5.03	-8.56	35.71	35.72
-4.94	-8.16	35.62	34.64
-3.96	-7.29	36.75	35.09
-3.87	-7.18	35.41	34.79
-3.79	-7.14	34.26	35.78
-3.32	-6.84	34.89	36.13
-3.22	-6.76	35.16	35.18
-3.19	-6.71	34.97	35.34

### 3.6. Interaction between wild-type enzyme and ginsenoside Rb1

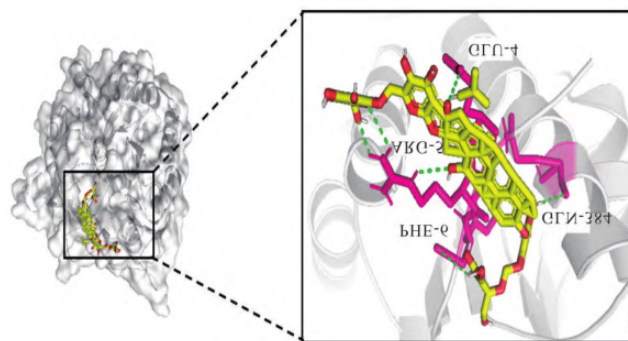
Molecular docking was performed between wild-type  $\beta$ -glucosidase and ginsenoside Rb1. The two-dimensional plan view of the docking results is shown in **Figure 4**.

**Figure 4.** Wild enzymes and ginsenoside Rb1.

It can be seen that ginsenoside Rb1 serves as the ligand molecule, and the green dashed lines represent hydrogen bonding interactions. The ligand molecule forms six hydrogen bonds with four amino acids (Glu4(A), Arg5(A), Phe6(A), Gln384(A)). The semicircles indicate hydrophobic interactions, and

ginsenoside Rb1 exhibits hydrophobic interactions with five amino acids (Glu166(A), Tyr295(A), Glu352(A), Trp399(A), Tyr415(A)).

Molecular docking was performed between wild-type  $\beta$ -glucosidase and ginsenoside Rb1, and the docking results are shown in **Figure 5**.

**Figure 5.** Interaction analysis diagram.

It can be observed that hydrogen bonding interactions are formed between the substrate and multiple active site residues <sup>[23,24]</sup>, which together constitute a hydrophobic cavity. The green dashed lines represent the hydrogen bonds formed between the amino acid residues and the small molecule ligand, with a total of 6 hydrogen bonds formed.

The sites occupied by GLU-4, ARG-5, PHE-6, and GLN-384 play a critical role in the binding of the substrate through hydrogen bonding with ginsenoside Rb1.

### 3.7. Interaction between mutant enzyme and ginsenoside Rb1

Molecular docking was performed between the mutant  $\beta$ -glucosidase and ginsenoside Rb1, and the two-dimensional plan view of the docking results is shown in **Figure 6**.

It can be seen that ginsenoside Rb1 serves as the ligand molecule, and the green dashed lines represent hydrogen bonding interactions. The ligand molecule forms 8 hydrogen bonds with 6 amino acids (Pro317(A), Asp318(A), His321(A), His358(A), Asp359(A), His368(A)). The semicircles indicate hydrophobic interactions, and ginsenoside Rb1 exhibits hydrophobic interactions with 7 amino acids (Leu319(A), Pro320(A), Thr322(A), His358(A), Ile367(A), Asp369(A),

Gln371(A)). Compared to the wild-type, the mutant enzyme exhibits stronger hydrophobic interactions with ginsenoside Rb1.

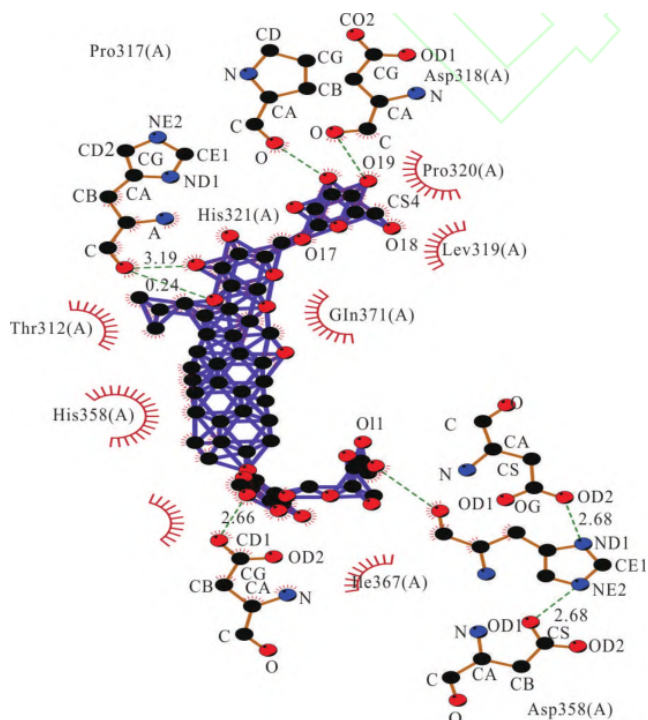


**Figure 6.** Mutase interacts with ginsenoside Rb1.

Molecular docking was further conducted between the mutant enzyme and ginsenoside Rb1, and the docking conformation is shown in **Figure 7**.

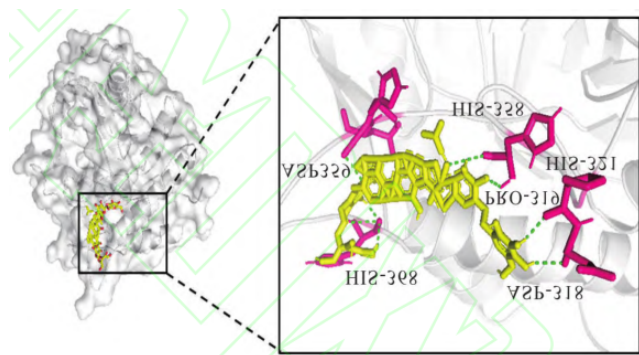


**Figure 7.** Hydrogen bonding interaction.

It can be observed that hydrogen bonding interactions are formed between the substrate and multiple active site residues, resulting in a total of 8 hydrogen bonds and a columnar hydrophobic cavity. The sites occupied by PRO-317, ASP-318, HIS-321, HIS-358, ASP-359, and HIS-368 play a key role in the binding of the substrate through hydrogen bonding with ginsenoside Rb1. The mutant enzyme forms 2 more hydrogen bonds with the ligand molecule than the wild-type enzyme, indicating a stronger binding ability between the mutant enzyme and ginsenoside Rb1, as well as the formation of stronger Van der Waals forces with the small molecule ligand.

## 4. Conclusion

The mutant  $\beta$ -glucosidase is a hydrophilic protein with increased hydrophilicity compared to the wild-type enzyme. Changes in the distribution of  $\alpha$ -helix and  $\beta$ -sheet regions within the protein enhance the stability of the mutant enzyme.

The binding structure of the complex between wild-type  $\beta$ -glucosidase and the small molecule ginsenoside Rb1 was obtained using molecular docking techniques. After mutation of the wild-type enzyme, the number of protein binding sites and hydrogen bonds increased, indicating that the mutant enzyme is more favorable for reacting with ginsenoside Rb1. As a member of the glycoside hydrolase family,  $\beta$ -glucosidase selectively hydrolyzes the ginsenoside glycosyl group during ginsenoside transformation.

## Funding

Shaanxi Provincial Natural Science Basic Research Program (Project No.: 2021JQ-672); Special Scientific Research Plan of Shaanxi Provincial Education Department (Project No.: 22JK0399)

**Disclosure statement**

The author declares no conflict of interest.

**References**

- [1] Zou G, Xin X, Liu J, et al., 2021, Study on Hydrolyzing of Tectoridin with  $\beta$ -Glucosidase. *Chinese Archives of Traditional Chinese Medicine*, 39(3): 40–43.
- [2] Zhang Y, Wang X, Wang S, et al., 2016, In Silico Investigation of the Association of the TRPM8 Ion Channel with the Pungent Flavor of Chinese Herbs. *Journal of Traditional Chinese Medical Sciences*, 3(4): 248–255.
- [3] Qiu Y, Xiang L, Wu C, et al., 2021, Study on the Interaction Between  $\beta$ -Lactoglobulin and Acrylamide. *The Light & Textile Industries of Fujian*, 2021(8): 2–5.
- [4] Phukoetphim N, Khongsay N, Laopaiboon P, et al., 2019, A Novel Aeration Strategy in Repeated-Batch Fermentation for Efficient Ethanol Production from Sweet Sorghum Juice. *Chinese Journal of Chemical Engineering*, 27(7): 1651–1658.
- [5] Matsuzawa T, Jo T, Uchiyama T, et al., 2016, Crystal Structure and Identification of a Key Amino Acid for Glucose Tolerance, Substrate Specificity, and Transglycosylation Activity of Metagenomic  $\beta$ -Glucosidase Td2F2. *The FEBS Journal*, 283(12): 2340–2353.
- [6] Hou L, Zhu F, 2021, Study on the Affinity Between  $\beta$ -Glucosidase and Substrate from *Aspergillus niger* 3.316. *Food Research and Development*, 42(7): 171–176.
- [7] Ni J, Xu G, Ni Y, 2021, Mapping of Key Catalytic Residues of *Lactobacillus brevis* L-Tyrosine Decarboxylase Using Site-Directed Mutagenesis. *Chinese Journal of Bioprocess Engineering*, 19(1): 32–39.
- [8] Dong K, Yang X, Zhao T, et al., 2016, Study on the Selectivity of Tetrahydropyrido[1,2-a]indolone Derivatives for GSK3 $\beta$  and CDK5 Using Molecular Simulation Methods. *Chinese Journal of Inorganic Chemistry*, 32(11): 1919–1930.
- [9] Ke J, Yu X, Zhao M, et al., 2022, The Hepatoprotective Mechanism of Reduning Based on Network Pharmacology and Molecular Docking. *Journal of Jiangxi Science & Technology Normal University*, 2022(6): 82–88.
- [10] Song C, Lyu B, Shi Z, et al., 2003, The Effects of Mutant Site G81R of RAB5A on RAB5A Function. *Acta Genetica Sinica*, 30(10): 967–972.
- [11] Qiao X, Su Y, Kang Y, et al., 2022, Cloning and Expression Analysis, Homology Modeling, and Molecular Docking of abaI Gene in *Acinetobacter baumannii*. *Chemical Research and Application*, 34(12): 2886–2893.
- [12] Zou Q, Zhong Q, Mao J, et al., 2023, Impact of Perturbation Schemes on the Ensemble Prediction in a Coupled Lorenz Model. *Advances in Atmospheric Sciences*, 40(3): 501–513.
- [13] Zhao P, Ma Y, Zhang N, et al., 2023, Study on Potence of Lobelia in Treatment of COVID-19 Based on Network Pharmacology and Molecular Docking. *Journal of North China University of Science and Technology (Natural Science Edition)*, 45(1): 109–118.
- [14] Feng Y, Qiu J, He J, et al., 2022, IL-18 and IL-18R Molecular Docking: Computational Development of a Simulation Method for Protein-Protein Interactions. *Chemistry Bulletin*, 85(12): 1510–1516.
- [15] Peng L, He S, Liu Y, et al., 2023, Rapid Determination of Glucose in Tobacco and Its Products by Enzymatic Reaction with Gray-Scale Analysis. *Physical Testing and Chemical Analysis (Part B: Chemical Analysis)*, 59(1): 29–33.
- [16] Zhang C, Wang J, Zhu L, et al., 2018, Effects of 1-Octyl-3-Methylimidazolium Nitrate on the Microbes in Brown Soil. *Journal of Environmental Sciences*, 67(5): 249–259.
- [17] Liu Y, Zhang D, Yao Y, et al., 2018, Mapping of IgG-Binding Epitopes on the A2 Chain of the Major Soybean Allergen 11S Globulin G2. *Food Science*, 39(18): 152–158.
- [18] Lei M, Su J, Li Z, et al., 2017, Homologous Modeling of the Three-Dimensional Structure of Cav1.2 Calcium Ion Channel

- and Its Application. Chinese Pharmacological Bulletin, 33(1): 12–23.
- [19] Yin G, Zhou X, Yao H, et al., 2022, Interaction Between Sivelestat Sodium and Elastase by Multispectra and Molecular Docking. Chinese Journal of Applied Chemistry, 39(6): 960–968.
- [20] Cao T, Wei X, Luo M, et al., 2022, Synthesis of 2-Sulfanylphenyl(alkyl)phenols and 10H-Phenothiazines Promoted by Iodosobenzene-Promoted Dehydrogenation-Oxidation Reaction. Organic Chemistry, 42(7): 2079–2088.
- [21] Feng Y, Huang X, Wen J, et al., 2023, Properties of Double-Ended Silohydroperfluoropolyether Polysiloxane in Nitrile Rubber. Fine Chemicals, 40(3): 673–679.
- [22] Li Y, Wang K, Hu H, et al., 2022, Molecular Dynamics Simulation of Properties of Cysteine-Rich Protein from Soybean. Journal of Jilin University (Science Edition), 60(5): 1202–1208.
- [23] Yang J, Zhou G, Zhan J, et al., 2023, Study on the Mechanism of Wuhe Dipsacus asper in Prevention and Treatment of Alzheimer's Disease Based on Network Pharmacology and Molecular Docking. Journal of Hubei Minzu University (Natural Science Edition), 41(1): 27–32.
- [24] Wei J, Tao Q, Chen X, et al., 2023, Exploring the Mechanism of Chuanxiong in Treating Rheumatoid Arthritis with Atherosclerosis Based on Network Pharmacology and Molecular Docking. Guangdong Chemical Industry, 50(5): 61–63.

**Publisher's note**

*Whioce Publishing remains neutral with regard to jurisdictional claims in published maps and institutional affiliations.*